Zigzag-Edged Polycyclic Aromatic Hydrocarbons from Benzo[m]tetraphene Precursors

Bo Yang+,[a] Yanwei Gu+,[a] Giuseppe M. Paternò,[b, c] Joan Teyssandier,[d] Ali Maghsoumi,[e] Alex J. Barker,[c] Kunal S. Mali,[d] Francesco Scotognella,[b] Steven De Feyter,[d] Matteo Tommasini,[e] Xinliang Feng,*[f, g] Akimitsu Narita,*[a] and Klaus Müllen*[a, h]

Abstract: A series of zigzag-edged polycyclic aromatic hydro-carbons (PAHs) (**Z1-Z3**) were synthesized from 2,12-dibromo-7,14-diphenyl-benzo[m]tetraphene (**9**) as a versatile building block. Their structures were unambiguously confirmed by laser desorption/ionization time-of-flight mass spectrometry, ^{1}H NMR, Raman, and Fourier-transformed infrared (FTIR) spectroscopies as well as scanning tunneling microscopy. The fingerprint vibrational modes were elucidated with theoretical support. The edge- and size-dependent optical properties were characterized by UV-Vis absorption and fluorescence spectroscopy and DFT calculations. Moreover, ultrafast tran-sient absorption spectroscopy revealed distinct modulation of the photophysical properties upon π-extension from **Z1** to **Z2**, the latter having a gulf edge.

Introduction

The studies of polycyclic aromatic hydrocarbons (PAHs) are evolving towards the development of organic materials for various applications such as sensing,[1] (opto−)electronics,[2] spintronics,[3] and energy storage,[4] considering their versatile electronic structures and physical properties. Many endeavors have been devoted to investigating size and edge effects on their electronic properties.[5] Typically, two types of edge structures have been considered, namely, zigzag and armchair (Figure 1a),[2b,6] while some other types, such as the cove and gulf, further contribute to the structural diversity.[7] Theoretical and experimental studies revealed the dramatically reduced optical energy gaps induced by zigzag edges, distinct from those PAHs possessing only armchair edges.[3b,8] Hence, the efficient synthesis of PAHs with zigzag edges and investigation of their structure-property relationships is of high relevance.

For the synthetic exploration of PAHs, the development of concise and efficient modular methods is desirable.[9] To this end, we have used 2,12-dibromo-7,14-diphenyl-benzo[m]tetraphene (**9**) as the building block, which is structur-ally related to the "U-shaped" monomers employed for the on-surface synthesis of zigzag graphene nanoribbons[7c,8c] (Fig-ure 1b). A long and branched alkyl chain is introduced on the skeleton to improve the solubility of the final PAH products. Through debromination or coupling reaction of **9**, followed by oxidative cyclodehydrogenation, a series of unprecedented PAHs with zigzag-edged structures can be obtained. Here we

[a] Dr. B. Yang,+ Dr. Y. Gu,+ Prof. A. Narita, Prof. K. Müllen
Max Planck Institute for Polymer Research
Ackermannweg 10, 55128 Mainz (Germany)
E-mail: narita@mpip-mainz.mpg.de
muellen@mpip-mainz.mpg.de

[b] Dr. G. M. Paternò, Prof. F. Scotognella
Physics Department, Politecnico di Milano
Piazza L. da Vinci 32, Milano 20133 (Italy)

[c] Dr. G. M. Paternò, Dr. A. J. Barker
Istituto Italiano di Tecnologia
Center for Nano Science and Technology
Milano, 20133 (Italy)

[d] Dr. J. Teyssandier, Dr. K. S. Mali, Prof. S. De Feyter
Department of Chemistry
Division of Molecular Imaging and Photonics
KU Leuven
Celestijnenlaan 200F, B-3001 Leuven (Belgium)

[e] Dr. A. Maghsoumi, Prof. M. Tommasini
Dipartimento di Chimica
Materiali e Ingegneria Chimica – Politecnico di Milano
Piazza Leonardo da Vinci, 32-20133 Milano (Italy)

[f] Prof. X. Feng
Center for Advancing Electronics and
Faculty of Chemistry and Food Chemistry
Technical University of Dresden
01062, Dresden (Germany)
E-mail: xinliang.feng@tu-dresden.de

[g] Prof. X. Feng
Max Planck Institute of Microstructure Physics
Weinberg 2, 06120 Halle (Germany)

[h] Prof. K. Müllen
Department of Chemistry
Johannes Gutenberg University Mainz
Duesbergweg 10–14, 55128 Mainz (Germany)

[+] These authors contributed equally to this work.

Supporting information for this article is available on the WWW under https://doi.org/10.1002/chem.202203981

This publication is part of a Special Collection on aromatic chemistry in collaboration with the "19th International Symposium on Novel Aromatic Compounds (ISNA-19)".

Chemistry–A European Journal

Research Article
doi.org/10.1002/chem.202203981

Chemistry Europe
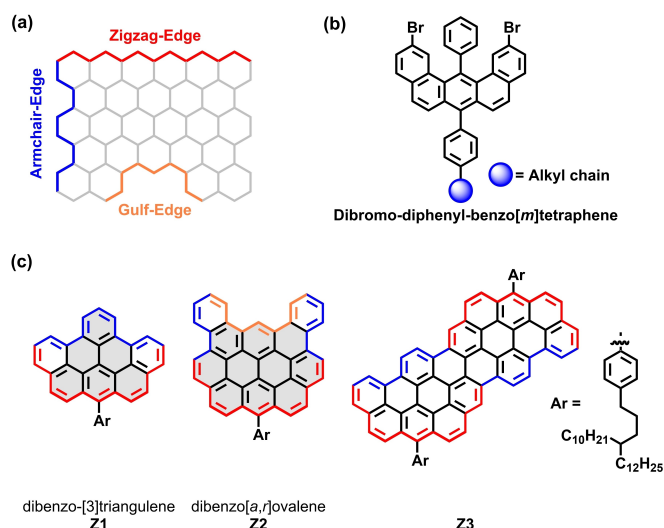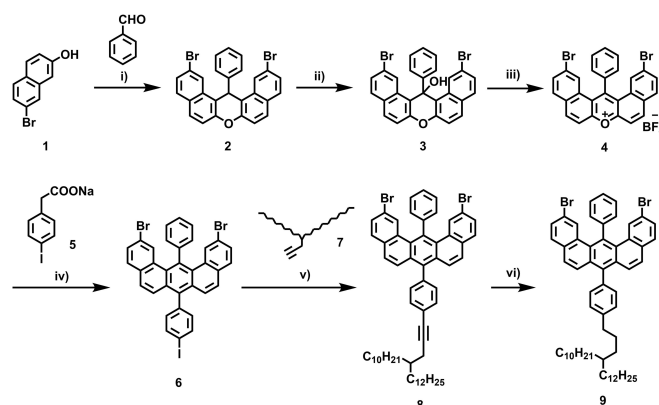European Chemical
Societies Publishing

Figure 1. (a) Edge structures of PAHs; (b) 2,12-dibromo-7,14-diphenyl-benzo[*m*]tetraphene with substituted alkyl chain; (c) Structures of partial zigzag-edged PAHs **Z1**-**Z3**.

Scheme 1. Synthetic route towards **DBDPBT 9**. Reagents and conditions: i) p-TsOH, neat, 125 °C, 86 %; ii) PbO$_2$, AcOH, 120 °C; iii) HBF$_4$ (50 % aq. solution), toluene/Ac$_2$O, 0 °C-r.t., 68 % in two steps; iv) Ac$_2$O, 150 °C, 35 %; v) PdCl$_2$(PPh$_3$)$_2$, CuI, Et$_3$N, THF, r.t., 86 %; vi) PtO$_2$, H$_2$ (5 bar), THF, 99 %.

report the synthesis and characterizations of three PAHs with zigzag edges, **Z1**, **Z2**, and **Z3** through this modular approach (Figure 1c). While **Z1** and **Z3** consist of zigzag and armchair edges, the latter being a dimer of the former, **Z2** possesses zigzag, armchair, and gulf edges. **Z1**-**Z3** were characterized by matrix-assisted laser desorption/ionization time-of-flight mass spectrometry (MALDI-TOF MS), NMR, FTIR, and Raman spectroscopies with theoretical supports, and scanning tunneling microscopy (STM). UV-Vis absorption and fluorescence spectra revealed significant red-shift upon π- extension from **Z1** to **Z2**, and then to **Z3**. Moreover, ultrafast transient absorption (TA) spectroscopy revealed significant differences in the photophysical properties of **Z1** and **Z2** despite their structural similarity.

Results and Discussion

Synthesis of "U-shaped" precursor 9

The synthesis of **9** was carried out through the condensation reaction between pyrylium salt **4** and sodium phenylacetate **5** as the key step (Scheme 1).[10] 2,12-Dibromo-14-phenyl-14H-dibenzo[*a,j*]xanthene (**2**) was initially prepared by condensation of 7-bromonaphthol (**1**) with two equivalents of benzaldehyde at 125 °C.[11] Oxidation of **2** with an excess amount of lead oxide in acetic acid at 120 °C afforded 2,12-dibromo-14-phenyl-14H-dibenzo[*a,j*]xanthen-14-ol (**3**), which was collected by precipitation and used for the next step without further purification. Subsequent treatment of **3** with tetrafluoroboric acid solution (50 wt.% aq.) provided pyrylium salt **4** in 68 % yield over two steps.[10] Next, pyrylium salt **4** was subjected to condensation with sodium 4-iodophenylacetate **5** at 150 °C, leading to the iodinated **6** in 34 % yield.[12] *Sonogashira* coupling of **6** with 11-(prop-2-yn-1-yl)tricosane (**7**) and subsequent hydrogenation[13]
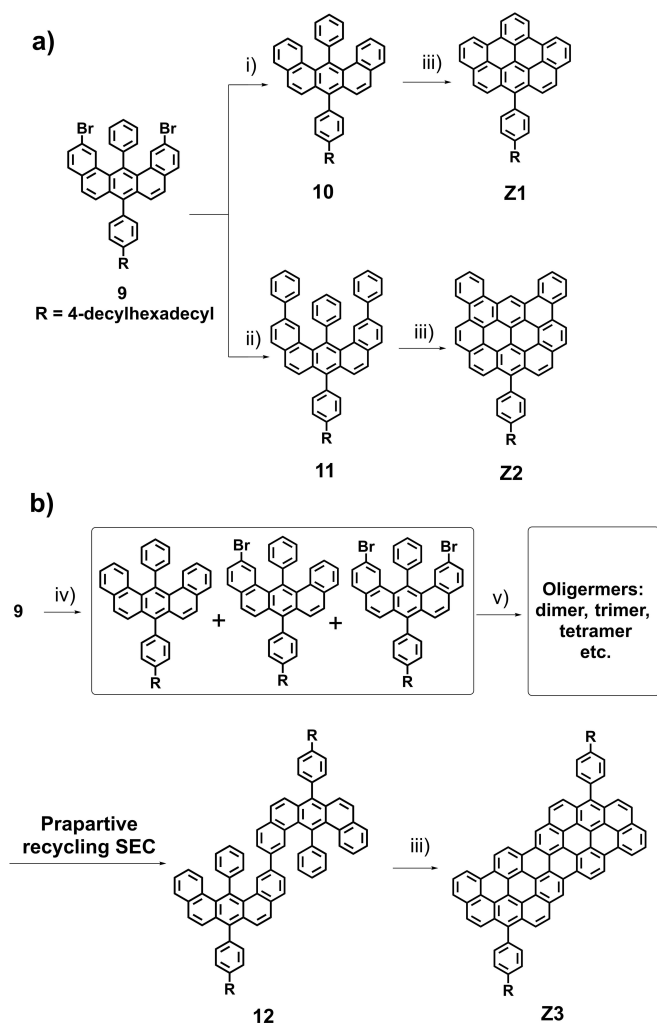
afforded compound **9** with branched 4-decylhexadecyl chain in 85 % yield over two steps.

Synthesis and characterization of Z1-Z3

For obtaining **Z1**, **Z2**, and **Z3**, the required precursors **10**, **11**, and **12**, respectively, were prepared from compound **9** (Scheme 2). First, debromination of **9** by treatment with two equivalents of *n*-butyllithium afforded compound **10** in 98 % yield. Subsequently, **10** could be readily transformed into the desired product **Z1** through the oxidative cyclodehydrogenation using 2,3-dichloro-5,6-dicyano-*p*-benzoquinone/trifluoroacetic acid (DDQ/TFA) (Scheme 2a) in 85 % yield.[14] MALDI-TOF MS analysis of **Z1** displayed a signal at $m/z = 790.25$, which was consistent with the expected value of 790.54 (Figure 2, black plot). Moreover, the isotopic distribution of **Z1** was in perfect agreement with the simulated pattern, which provided strong evidence for the formation of **Z1**.

Precursor **11** was next prepared through the *Suzuki* coupling of **9** with phenylboronic acid in 71 % yield. The cyclodehydrogenation of **12** with DDQ/TFA afforded target **Z2** in 81 % yield. On the other hand, the synthesis of **Z3** was achieved in four steps (Scheme 2b): 1) compound **9** was treated with one equivalent of *n*-butyllithium to give a mixture of **9**, **10**, and their mono-bromo derivative; 2) This mixture was subjected to a *Yamamoto* coupling to furnish a mixture of oligomers, including dimer **12**, trimer, and tetramer; 3) The oligomers were then separated by preparative recycling size-exclusion chromatography (SEC), providing dimer **12** in 16 % yield; 4) The subsequent oxidative cyclodehydrogenation of **12** gave **Z3**. Similar to **Z1**, MALDI-TOF MS analysis of **Z2** and **Z3** exhibited mass peaks at $m/z = 938.66$ and 1575.03 in line with the theoretical molecular mass of 938.58 and 1575.05, respectively (Figure 2, blue and red plots). Their isotopic distributions were also in agreement with the simulated patterns, which validated the successful formation of **Z2** and **Z3**.

Chemistry–A European Journal

Research Article
doi.org/10.1002/chem.202203981

Chemistry
Europe
European Chemical
Societies Publishing

Scheme 2. Synthetic routes to PAHs: a) **Z1** and **Z2**; b) **Z3**. Reagents and conditions: i) 2.0 equiv. of n-BuLi, THF, −78 °C, then MeOH, 98 %; ii) phenylboronic acid, Pd(PPh₃)₄, K₂CO₃, toluene/H₂O, reflux, 71 %; iii) DDQ/TFA, dichloromethane, 0 °C - r.t., **Z1**: 85 %; **Z2**: 81 %; **Z3**: 47 %; iv) 1.0 equiv. of n-BuLi, THF, −78 °C, then MeOH; v) Ni(COD)₂, 2,2′-bipyrindine, COD, 60–80 °C, **12**: 16 % in two steps. COD: 1,5-cyclooctadiene.

Figure 2. Reflectron-mode MALDI-TOF mass spectra of **Z1**, **Z2**, and **Z3** (solid-state sample preparation, matrix: TCNQ); inserted: isotopic distribution obtained by MALDI-TOF MS measurements in perfect agreement with the simulation.

Figure 3. ^{1}H NMR spectra of **Z1** in dichloromethane-d_2 at 25 °C; inset: The assignment of aliphatic and aromatic protons of **Z1**.

Generally, extended PAHs suffer from strong aggregation in solution, which results in the broadening of peaks in ^{1}H NMR spectra. Nevertheless, the well-resolved ^{1}H NMR spectrum of **Z1** could be recorded at room temperature in dichloromethane-d_2 (Figure 3), and those of **Z2** and **Z3** at 393 K in 1,1,2,2-tetrachloroethane-d_2 (see Supporting Information, Figure S26–27). Because of the extended π-system, some proton signals on the aromatic backbone appeared downfield and shifted to a range of $\delta = 8.0$–9.5 ppm. Moreover, the signal of the proton at the "gulf" position of **Z2** was more strongly downfield shifted to $\delta = 10.4$ ppm, which indicates the intense deshielding effect by neighboring aromatic rings. With the help of 2D H–H Correlation Spectroscopy (COSY) NMR, aliphatic and aromatic signals of **Z1** and **Z2** could be assigned, further verifying the successful synthesis of the model compounds (see Supporting Information, Figure S4).
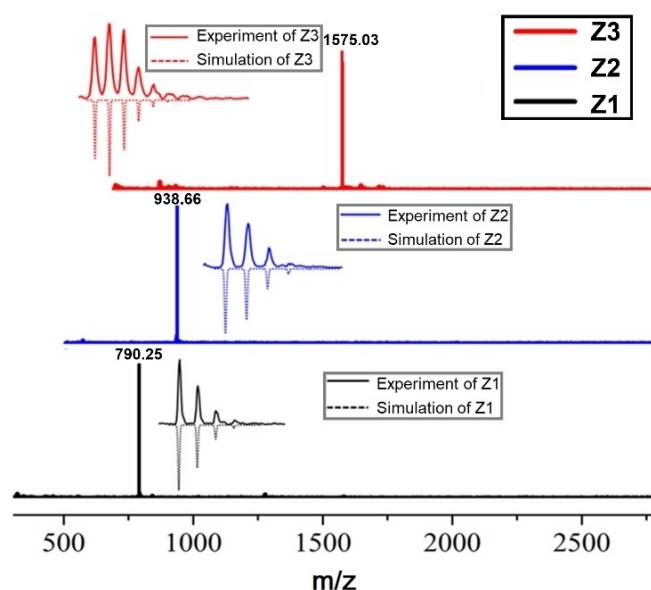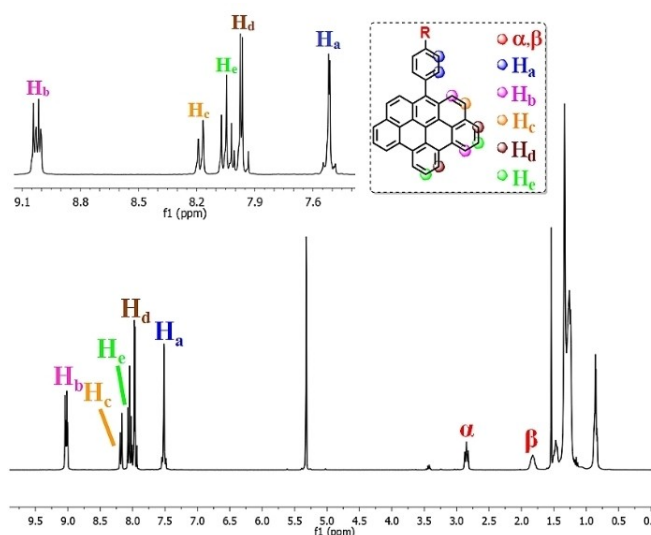
Raman and Fourier-transform infrared analyses of Z1 and Z2

Raman and FTIR spectra of **Z1** and **Z2** were studied to obtain insights into the vibrational modes of such PAHs with zigzag, armchair, and gulf edges (Figure 4). The Raman spectra of PAHs are generally dominated by collective C–C stretching vibrations of the honeycomb structure, which are named D and G in the literature.[15] Correspondingly, the Raman spectra of **Z1** and **Z2** exhibit these characteristic signals around 1300 cm^{-1} and 1600 cm^{-1} (Figure 4a). The multiplicity of D and G signals is a

Chemistry–A European Journal

Research Article
doi.org/10.1002/chem.202203981

Chemistry
Europe
European Chemical
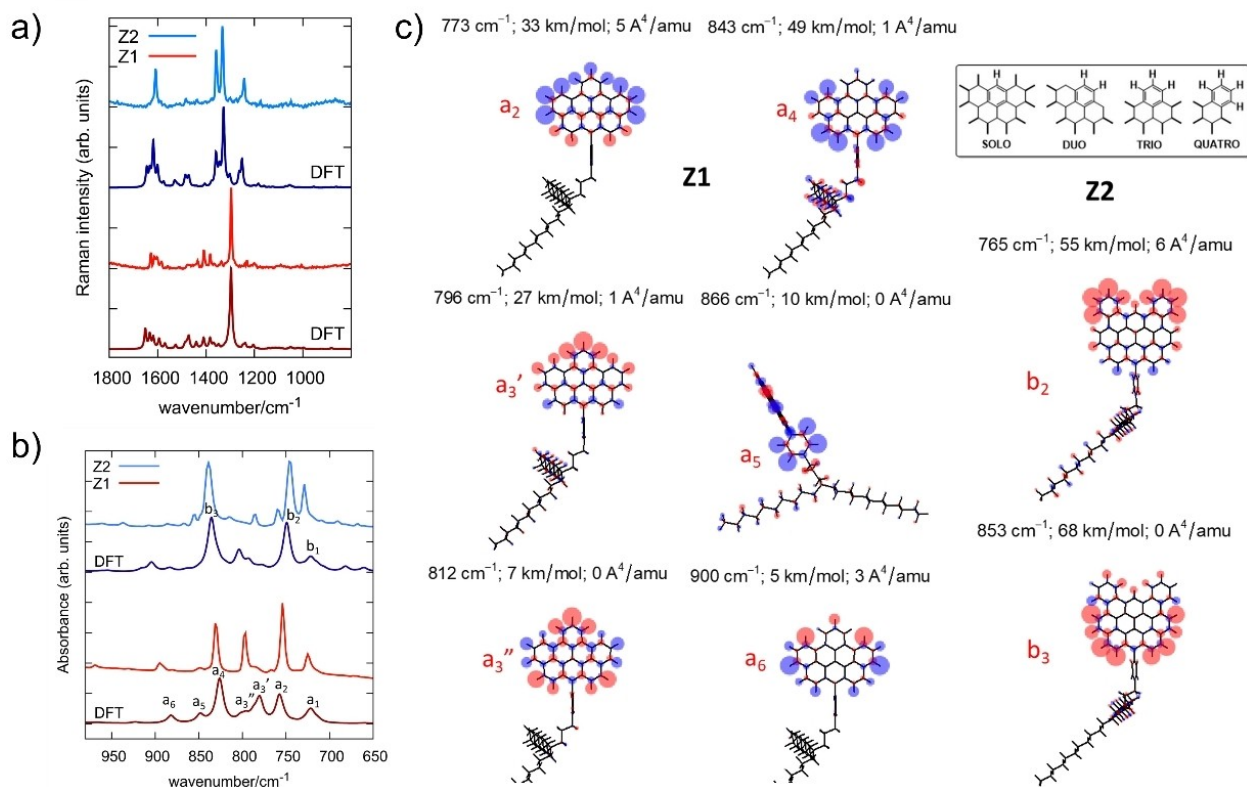Societies Publishing

Figure 4. (a) Experimental (top traces) and simulated (bottom traces, frequency scaled by 0.98) FT-Raman spectra of **Z1** and **Z2** (1064 nm excitation). (b) Experimental and simulated FTIR spectra of **Z1** and **Z2** in the fingerprint out-of-plane CH bending region. Simulated spectra have been frequency scaled by 0.98 and are reported below each corresponding experimental spectrum. (c) Representation of normal modes associated with the FTIR spectra features labeled in panel b. The size of blue/red circles on the molecular sketches is proportional to positive/negative nuclear displacements along the out-of-plane direction. Inset: Representation of SOLO, DUO, TRIO, and QUATRO.

typical property of PAHs resulting from the coupling of characteristic collective C–C stretching coordinates with the in-plane C–H bending vibrations at the edge of the molecule.[16] Even though it is difficult to identify specific edge markers, i.e., peaks originating from specific edge structures, it is clear from the comparison of the Raman spectra of **Z1** and **Z2** that the manifold of peaks in the D and G regions, as a whole, can be regarded as the fingerprint of the molecular structures. DFT calculations on **Z1** and **Z2** provide simulated Raman spectra which nicely correlate with the experimental results and allow the identification of all minor vibrations involving different normal modes related to collective breathing modes and ring stretching modes. Inspection of the normal modes associated with the intense Raman peaks reveals the expected nuclear displacements for D and G modes (see Supporting Information, Figure S1).

The infrared signals of PAHs in the CH out-of-plane (*opla*) bending region (980–650 cm^{-1} range) are informative of the molecular structure and edge topology.[17] The comparison of the theoretical and experimental spectra of **Z1** and **Z2** shows a good agreement, as reported in Figure 4b. Deviations between the theory and the experiment are presumably due to the role of intermolecular interactions in the solid state since the calculations were performed for isolated molecules. The pres-

ence of alkyl substituents could also induce an effect on the signals through contributions arising from the manifold of possible conformers. Nevertheless, to limit the computational cost, only the fully *trans*-planar conformations of the substituents were considered in the DFT calculations (see Supporting Information, Figure S2) and we focused on the CH-*opla* markers. In the IR spectra of Figure 4b, the a_1 feature of **Z1** can be assigned to the rocking modes of the alkyl chains; b_1 is the rocking mode in **Z2**. The remaining bands labeled in the FTIR spectra of Figure 4b are all due to *opla* vibrations of CH bonds. Several signals (i.e., a_2, a_3', a_3'', a_4, and a_6 in **Z1** and b_2 and b_3 in **Z2**) are characteristic of the specific edge configurations, whereas the weak a_5 band is assigned to the lateral phenyl substitution.

Adopting the mode naming described in the literature,[17–18] and with reference to the pattern of the normal modes, the b_2 signal in **Z2** can be described as QUATRO and b_3 as DUO (Figure 4c, insert). The a_2 and a_3' bands of **Z1** can be described as TRIO and a_4 as DUO. The remaining two modes (a_3'', a_6) have a more complex pattern of in-phase/out-of-phase CH-*opla* contributions. All these Raman and FTIR characterizations of **Z1** and **Z2** show good agreement with corresponding DFT calculations, providing additional structural evidence and also

Chemistry–A European Journal

Research Article
doi.org/10.1002/chem.202203981

Chemistry
Europe
European Chemical
Societies Publishing

marking the strength of vibrational spectroscopy for precisely characterizing PAHs with different structures.

Scanning tunneling microscopy analysis of Z3

Except for the structural confirmation through ^{1}H NMR measurement, the STM analysis of **Z3** also allowed the visualization of its molecular and self-assembled structures at the solution-graphite interface.[19] **Z3** was selected for STM analysis due to its large footprint which is expected to stabilize the self-assembled monolayers via π-π interactions with the graphite surface. Figure 5a displays a typical STM image of the **Z3** monolayer formed at the highly oriented pyrolytic graphite (HOPG)/1,2,4-trichlorobenzene (TCB) interface, which displays rows of bright rectangular units stacked end-to-end. Each rectangular unit corresponds to the aromatic backbone of a single **Z3** molecule.

The dimensions of the aromatic core extracted from calibrated STM images (length ~2.3 nm, width ~1.1 nm) are in good agreement with those obtained from a model optimized by molecular mechanics (Figure 5b). The bright rows are periodically separated by relatively darker troughs. The distance between the bright adjacent rows (unit cell vector b) indicates that the darker region hosts the tetradecyl chain, i.e., the shorter decyl branch of the 4-decylhexadecyl group. The longer dodecyl arm may be partially adsorbed or alternatively back-folded in the supernatant solution. The alkyl chains could not be resolved, possibly in view of their mobility on the time scale of STM imaging. The molecular model displayed in Figure 5b depicts the arrangement of **Z3** molecules within the self-assembled network. The empty regions in the molecular model could be occupied by the partially adsorbed dodecyl arm of the chain or by mobile TCB molecules (both not shown in the molecular model for the sake of clarity).
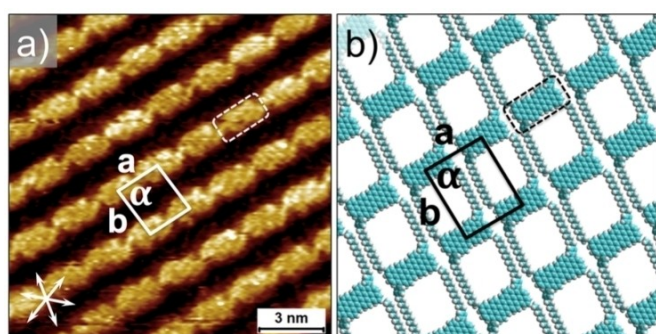
Optical properties of Z1-Z3

The optical properties of **Z1-Z3** were studied using UV-vis absorption and photoluminescence spectroscopies in THF solutions (Figure 6a). UV-vis absorption spectra of three compounds show distinct bathochromic shifts with increasing size of the π-conjugated aromatic cores, exhibiting the absorption maxima at 355, 374, and 412 nm, which are attributed to the p-, β-, and β′-band based on Clar's notation and correspond to HOMO→LUMO, HOMO→LUMO+1, and HOMO-1→LUMO+1.[20] The time-dependent (TD) DFT calculations (see Supporting Information, Table S1-S3) support this attribution that the maximum absorption band of each molecule can be assigned to H-1→L+1 (52%) & H→L (44%) for **Z1**, H-1→L (45%) & H→L+1 (47%) for **Z2**, and H-1→L+1 (90%) for **Z3**, where H and L stand for HOMO and LUMO, respectively. Although the α-band (HOMO-1→LUMO) is observed in UV-vis spectra of **Z1** (378 nm) and **Z3** (500 nm), it cannot be found in the recorded UV-vis spectrum of **Z2** because of its weak oscillator strength (0.0002, see Supporting Information, Table S2) as well as the overlap
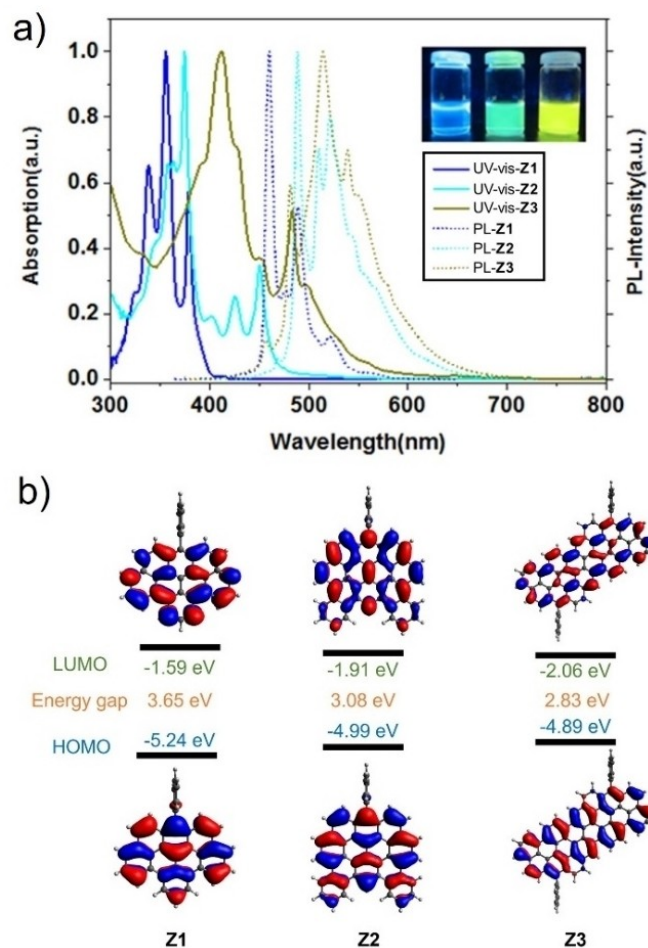
Figure 6. (a) Normalized UV-vis absorption and photoluminescence spectra of **Z1**, **Z2**, and **Z3** in THF; inserted: photographs of **Z1**, **Z2**, and **Z3** in THF under 254 nm UV light. (b) DFT-calculated molecular orbitals, and energy diagrams of **Z1-Z3**. The branched 4-decylhexadecyl chain was omitted to simplify the calculation.

Figure 5. STM characterization of the compound **Z3**. (a) STM image showing a self-assembled network of **Z3** formed at the TCB/HOPG interface ($C_{Z3} = 6.3 \times 10^{-5}$ M). The dashed rectangle highlights the aromatic backbone of a single **Z3** molecule. The graphite symmetry axes are displayed in the lower left corner. The unit cell is overlaid on the STM image and the parameters are a = 2.3 ± 0.2 nm, b = 2.7 ± 0.1 nm, α = 84.5 ± 3°. Imaging parameters: I_{set} = 75 pA, V_{bias} = −1.125 V. (b) Molecular model showing the arrangement of **Z3** molecules within the self-assembled network. The dodecyl arm of the branched chain is plausibly backfolded in the super-natant liquid phase and is not shown in the molecular model.

Chemistry–A European Journal

Research Article
doi.org/10.1002/chem.202203981

Chemistry Europe
European Chemical
Societies Publishing

with the strong p-band, which is split into three peaks by vibronic coupling, similar to our previous observation for the hexabenzocoronene with partial zigzag edges.[8e,21]

The HOMO-LUMO energy gaps of **Z1**-**Z3** were calculated to be 3.65, 3.08, and 2.83 eV (Figure 6b) based on the DFT method, which agreed with the bathochromic shifts of the absorption maxima.

The excitation spectra of three PAHs were also recorded, which were in good agreement with their absorption spectra, corroborating the purity of the obtained samples (see Supporting Information, Figure S3). **Z1**, **Z2**, and **Z3** display fluorescence with emission maxima at 459, 488, and 514 nm, respectively, under excitation at their absorption maxima (Figure 6). Their photoluminescence spectra revealed many sharp bands, which apparently pointed to the symmetry-forbidden transition from the first excited singlet state to the ground state, similar to that of the previously reported PAHs with partial zigzag edges.[22]

Transient absorption spectroscopy of Z1 and Z2

The ultrafast transient absorption (TA) spectroscopy was employed to gain a deeper insight into the photophysical properties of **Z1** and **Z2** (Figure 7), which showed distinct static optical spectra despite the structural similarity. The structure-property correlation in larger PAHs has been investigated with this method,[23] especially indicating the promoted occurrence of stimulated emission (SE) signal and gain properties along with the introduction/extension of the zigzag edges.[8e,24] Nevertheless, the precise structure-property relationship is still largely unclear, for which **Z1** and **Z2**, sharing the same zigzag-edged (sub)structure, offer an intriguing comparison. To minimize the intermolecular aggregation, **Z1** and **Z2** were blended into a polystyrene solution (40 mg/mL in toluene) with a concentration of 0.1 mg/mL for the TA measurements. Although the signal intensity of **Z1** is relatively lower than that of **Z2** due to the reduced oscillator strength at the selected excitation wavelength (400 nm), **Z1** exhibits a broad negative signal that can be associated with the excited-state absorption ($S_1 \rightarrow S_i$), with possibly a hint of positive SE signal at 470 nm (0'-0 transition) that is strongly overwhelmed by the negative absorption signal. In contrast, **Z2** displays a positive signal centered around 500 nm, which can be attributed to SE (0-0') transition and is clearly more prominent than in **Z1**. Although the damping of SE in **Z2** is ultrafast and occurs in ~300 fs, this observation indicates that the zigzag edge alone does not bring about the occurrence of SE, which is caused by the π-extension, forming a gulf edge, in this case of **Z1** vs. **Z2**. This phenomenon could be attributed to an increased electron localization and reduced non-radiative recombination upon the π-extension, while the possible appearance of hypothesized localized topological emissive states[25] is still under investigation with other PAH systems.
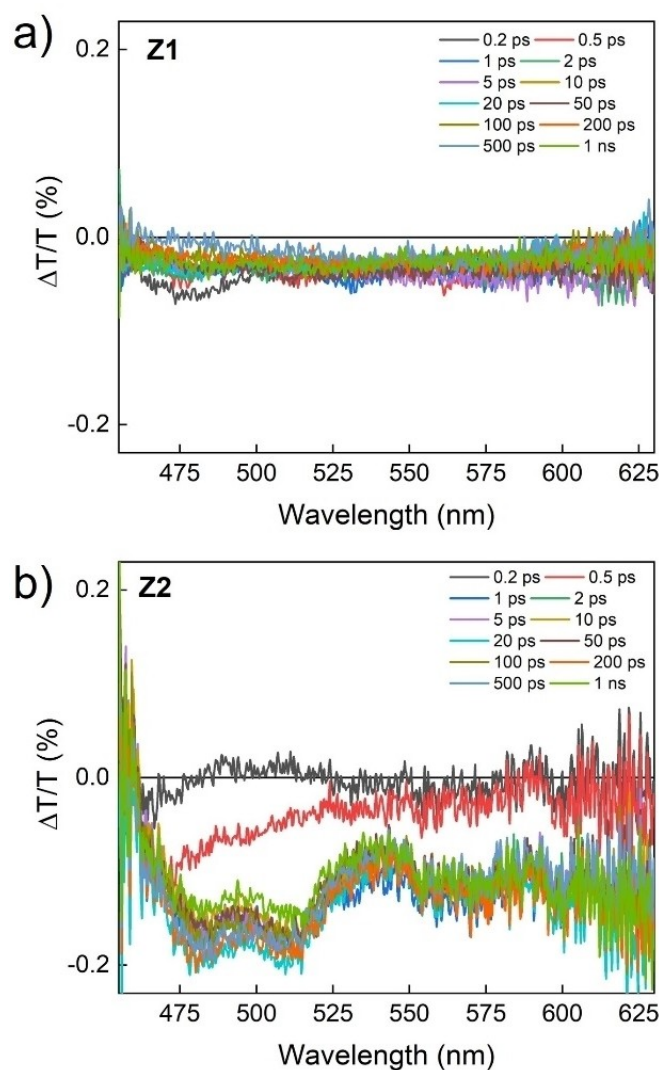

Figure 7. TA spectra as a function of pump-probe delay for (a) **Z1** and (b) **Z2** suspended in a polystyrene solution (40 mg/mL in toluene) with a concentration of 0.1 mg/mL. The excitation wavelength was 400 nm for both molecules.

Conclusion

In summary, we synthesized three zigzag-edged PAHs, **Z1**, **Z2**, and **Z3**, from a common "U-shaped" intermediate compound **9**. The most prominent feature of the resultant PAHs is edge- and size-dependent electronic properties, and their optical energy gaps moderately lower from 3.19 eV to 2.29 eV upon the π-extension. This work offers a deeper understanding of the structure-property relationships of PAHs with the common zigzag-edged (sub)structure, revealing the modulation of vibrational, optoelectronic, and photophysical properties. Furthermore, we observed the formation of oligomers, such as trimer and tetramer during the homo-coupling reaction of **9**, which can be potentially extended to the synthesis of related graphene nanoribbons with partial zigzag edges.[7d,26]

Chemistry–A European Journal

Research Article
doi.org/10.1002/chem.202203981

Chemistry Europe
European Chemical
Societies Publishing

Experimental Section

Essential Experimental Procedures/Data are available in the Supporting Information material of this article.

Conflict of Interest

The authors declare no conflict of interest.

Data Availability Statement

The data that support the findings of this study are available from the corresponding author upon reasonable request.

[1] a) J. Liu, Z. Liu, C. J. Barrow, W. Yang, *Anal. Chim. Acta* **2015**, *859*, 1–19; b) N. Bachar, L. Liberman, F. Muallem, X. Feng, K. Mullen, H. Haick, *ACS Appl. Mater. Interfaces* **2013**, *5*, 11641–11653; c) W. Qu, W. Yuan, M. Li, Y. Chen, *Chin. Chem. Lett.* **2021**, *32*, 3837–3840.

[2] a) L. A. Ponomarenko, F. Schedin, M. I. Katsnelson, R. Yang, E. W. Hill, K. S. Novoselov, A. K. Geim, *Science* **2008**, *320*, 356–358; b) J. Wu, W. Pisula, K. Müllen, *Chem. Rev.* **2007**, *107*, 718–747; c) X.-Y. Wang, X. Yao, K. Müllen, *Sci. China Chem.* **2019**, *62*, 1099–1144; d) C. Chen, M. W. Wang, X. Y. Zhao, S. Yang, X. Y. Chen, X. Y. Wang, *Angew. Chem. Int. Ed.* **2022**, *61*, e202200779; e) W. Li, C. Z. Du, X. Y. Chen, L. Fu, R. R. Gao, Z. F. Yao, J. Y. Wang, W. Hu, J. Pei, X. Y. Wang, *Angew. Chem. Int. Ed.* **2022**, *61*, e202201464; f) C. Zong, X. Zhu, Z. Xu, L. Zhang, J. Xu, J. Guo, Q. Xiang, Z. Zeng, W. Hu, J. Wu, R. Li, Z. Sun, *Angew. Chem. Int. Ed.* **2021**, *60*, 16230–16236; *Angew. Chem.* **2021**, *133*, 16366–16372; g) R. Muñoz-Mármol, V. Bonal, G. M. Paternò, A. M. Ross, P. G. Boj, J. M. Villalvilla, J. A. Quintana, F. Scotognella, C. D'Andrea, S. Sardar, G. Lanzani, Y. Gu, J. Wu, M. A. Díaz-García, *Nanomaterials* **2020**, *10*; h) M. Yang, I. S. Park, T. Yasuda, *J. Am. Chem. Soc.* **2020**, *142*, 19468–19472; i) K. Liu, Z. Jiang, R. A. Lalancette, X. Tang, F. Jakle, *J. Am. Chem. Soc.* **2022**, *144*, 18908–18917.

[3] a) Z. Sun, Q. Ye, C. Chi, J. Wu, *Chem. Soc. Rev.* **2012**, *41*, 7857–7889; b) W. Zeng, J. Wu, *Chem* **2021**, *7*, 358–386; c) Q. Xiang, J. Guo, J. Xu, S. Ding, Z. Li, G. Li, H. Phan, Y. Gu, Y. Dang, Z. Xu, Z. Gong, W. Hu, Z. Zeng, J. Wu, Z. Sun, *J. Am. Chem. Soc.* **2020**, *142*, 11022–11031; d) Y. Guo, S. Ding, N. Zhang, Z. Xu, S. Wu, J. Hu, Q. Xiang, Z. Y. Li, X. Chen, S. Sato, J. Wu, Z. Sun, *J. Am. Chem. Soc.* **2022**, *144*, 2095–2100; e) J. J. Dressler, M. M. Haley, *J. Phys. Org. Chem.* **2020**, *33*, e4114; f) Z. X. Chen, Y. Li, F. Huang, *Chem* **2021**, *7*, 288–332; g) H. Zhang, M. Pink, Y. Wang, S. Rajca, A. Rajca, *J. Am. Chem. Soc.* **2022**, *144*, 19576–19591.

[4] a) Y. Gu, Z. Qiu, K. Mullen, *J. Am. Chem. Soc.* **2022**, *144*, 11499–11524; b) J. Qu, X.-X. Dai, J.-S. Cui, R.-X. Chen, X. Wang, Y.-H. Lin, R. Verduzco, H.-L. Wang, *J. Mater. Chem. A* **2021**, *9*, 16554–16564; c) D. Kong, T. Cai, H. Fan, H. Hu, X. Wang, Y. Cui, D. Wang, Y. Wang, H. Hu, M. Wu, Q. Xue, Z. Yan, X. Li, L. Zhao, W. Xing, *Angew. Chem. Int. Ed.* **2022**, *61*, e202114681.

[5] a) M. Y. Han, B. Özyilmaz, Y. Zhang, P. Kim, *Phys. Rev. Lett.* **2007**, *98*, 206805; b) C. Tao, L. Jiao, O. V. Yazyev, Y.-C. Chen, J. Feng, X. Zhang, R. B. Capaz, J. M. Tour, A. Zettl, S. G. Louie, H. Dai, M. F. Crommie, *Nat. Phys.* **2011**, *7*, 616–620; c) O. V. Yazyev, *Acc. Chem. Res.* **2013**, *46*, 2319–2328; d) X. Xu, K. Müllen, A. Narita, *Bull. Chem. Soc. Jpn.* **2020**, *93*, 490–506.

[6] a) Y. Gu, X. Wu, T. Y. Gopalakrishna, H. Phan, J. Wu, *Angew. Chem. Int. Ed.* **2018**, *57*, 6541–6545; *Angew. Chem.* **2018**, *130*, 6651–6655; b) Y. Gu, Y. G. Tullimilli, J. Feng, H. Phan, W. Zeng, J. Wu, *Chem. Commun.* **2019**, *55*, 5567–5570; c) M. Franceschini, M. Crosta, R. R. Ferreira, D. Poletto, N. Demitri, J. P. Zobel, L. Gonzalez, D. Bonifazi, *J. Am. Chem. Soc.* **2022**, *144*, 21470–21484; d) A. Berezin, N. Biot, T. Battisti, D. Bonifazi, *Angew. Chem. Int. Ed.* **2018**, *57*, 8942–8946; *Angew. Chem.* **2018**, *130*, 9080–9084.

[7] a) Y. Gu, R. Muñoz-Mármol, S. Wu, Y. Han, Y. Ni, M. A. Díaz-García, J. Casado, J. Wu, *Angew. Chem. Int. Ed.* **2020**, *59*, 8113–8117; *Angew. Chem.* **2020**, *132*, 8190–8194; b) Y. Gu, V. Vega-Mayoral, S. Garcia-Orrit, D. Schollmeyer, A. Narita, J. Cabanillas-Gonzalez, Z. Qiu, K. Mullen, *Angew. Chem. Int. Ed.* **2022**, *61*, e202201088; c) P. P. Shinde, J. Liu, T. Dienel, O. Gröning, T. Dumslaff, M. Mühlinghaus, A. Narita, K. Müllen, C. A. Pignedoli, R. Fasel, P. Ruffieux, D. Passerone, *Carbon* **2021**, *175*, 50–59; d) J. Liu, B.-W. Li, Y.-Z. Tan, A. Giannakopoulos, C. Sanchez-Sanchez, D. Beljonne, P. Ruffieux, R. Fasel, X. Feng, K. Müllen, *J. Am. Chem. Soc.* **2015**, *137*, 6097–6103; e) Y. Yano, N. Mitoma, H. Ito, K. Itami, *J. Org. Chem.* **2020**, *85*, 4–33.

[8] a) K. Nakada, M. Fujita, G. Dresselhaus, M. S. Dresselhaus, *Phys. Rev. B* **1996**, *54*, 17954–17961; b) Y.-W. Son, M. L. Cohen, S. G. Louie, *Phys. Rev. Lett.* **2006**, *97*, 216803; c) P. Ruffieux, S. Wang, B. Yang, C. Sanchez-Sanchez, J. Liu, T. Dienel, L. Talirz, P. Shinde, C. A. Pignedoli, D. Passerone, T. Dumslaff, X. Feng, K. Mullen, R. Fasel, *Nature* **2016**, *531*, 489–492; d) S. Mishra, X. Yao, Q. Chen, K. Eimre, O. Gröning, R. Ortiz, M. Di Giovannantonio, J. C. Sancho-García, J. Fernández-Rossier, C. A. Pignedoli, K. Müllen, P. Ruffieux, A. Narita, R. Fasel, *Nat. Chem.* **2021**, *13*, 581–586; e) T. Dumslaff, Y. Gu, G. M. Paterno, Z. Qiu, A. Maghsoumi, M. Tommasini, X. Feng, F. Scotognella, A. Narita, K. Mullen, *Chem. Sci.* **2020**, *11*, 12816–12821.

[9] a) A. S. Scholz, J. G. Massoth, M. Bursch, J.-M. Mewes, T. Hetzke, B. Wolf, M. Bolte, H.-W. Lerner, S. Grimme, M. Wagner, *J. Am. Chem. Soc.* **2020**, *142*, 11072–11083; b) J.-J. Zhang, L. Yang, F. Liu, Y. Fu, J. Liu, A. A. Popov, J. Ma, X. Feng, *Angew. Chem. Int. Ed.* **2021**, *60*, 25695–25700; *Angew. Chem.* **2021**, *133*, 25899–25904; c) C.-W. Ju, B. Li, L. Li, W. Yan, C. Cui, X. Ma, D. Zhao, *J. Am. Chem. Soc.* **2021**, *143*, 5903–5916; d) X. Yin, K. Zheng, Z. Jin, M. Horst, Y. Xia, *J. Am. Chem. Soc.* **2022**, *144*, 12715–12724; e) H. Xin, J. Li, R. Q. Lu, X. Gao, T. M. Swager, *J. Am. Chem. Soc.* **2020**, *142*, 13598–13605.

[10] a) D. Wu, X. Feng, M. Takase, M. C. Haberecht, K. Müllen, *Tetrahedron* **2008**, *64*, 11379–11386; b) D. Wu, W. Pisula, M. C. Haberecht, X. Feng, K. Müllen, *Org. Lett.* **2009**, *11*, 5686–5689.

[11] M. Khodaei, A. Khosropour, H. Moghannian, *Synlett* **2005**, *2005*, 0955–0958.

[12] S. Klyatskaya, N. Dingenouts, C. Rosenauer, B. Müller, S. Höger, *J. Am. Chem. Soc.* **2006**, *128*, 3150–3151.

[13] L. Dössel, L. Gherghel, X. Feng, K. Müllen, *Angew. Chem. Int. Ed.* **2011**, *50*, 2540–2543; *Angew. Chem.* **2011**, *123*, 2588–2591.

[14] a) J. D. Chen, H. Y. Lu, C. F. Chen, *Chem. Eur. J.* **2010**, *16*, 11843–11846; b) D. J. Jones, B. Purushothaman, S. Ji, A. B. Holmes, W. W. Wong, *Chem. Commun.* **2012**, *48*, 8066–8068.

[15] a) C. Castiglioni, M. Tommasini, G. Zerbi, *Phil. Trans. R. Soc. A* **2004**, *362*, 2425–2459; b) A. C. Ferrari, D. M. Basko, *Nat. Nanotechnol.* **2013**, *8*, 235–246.

[16] F. Negri, C. Castiglioni, M. Tommasini, G. Zerbi, *J. Phys. Chem. A* **2002**, *106*, 3306–3317.

Chemistry–A European Journal

Research Article
doi.org/10.1002/chem.202203981

Chemistry Europe
European Chemical
Societies Publishing

[17] M. Tommasini, A. Lucotti, M. Alfè, A. Ciajolo, G. Zerbi, *Spectrochim. Acta Part A* **2016**, *152*, 134–148.

[18] A. Centrone, L. Brambilla, T. Renouard, L. Gherghel, C. Mathis, K. Müllen, G. Zerbi, *Carbon* **2005**, *43*, 1593–1609.

[19] K. S. Mali, J. Adisoejoso, E. Ghijsens, I. De Cat, S. De Feyter, *Acc. Chem. Res.* **2012**, *45*, 1309–1320.

[20] E. Clar, *Polycyclic Hydrocarbons*, Springer, Berlin, Heidelberg, **1964**.

[21] T. Dumslaff, B. Yang, A. Maghsoumi, G. Velpula, K. S. Mali, C. Castiglioni, S. De Feyter, M. Tommasini, A. Narita, X. Feng, K. Mullen, *J. Am. Chem. Soc.* **2016**, *138*, 4726–4729.

[22] a) M. Kastler, J. Schmidt, W. Pisula, D. Sebastiani, K. Müllen, *J. Am. Chem. Soc.* **2006**, *128*, 9526–9534; b) X. Feng, J. Wu, M. Ai, W. Pisula, L. Zhi, J. P. Rabe, K. Müllen, *Angew. Chem. Int. Ed.* **2007**, *46*, 3033–3036; *Angew. Chem.* **2007**, *119*, 3093–3096; c) R. Rieger, K. Müllen, *J. Phys. Org. Chem.* **2010**, *23*, 315–325.

[23] G. M. Paternò, Goudappagouda, Q. Chen, G. Lanzani, F. Scotognella, A. Narita, *Adv. Opt. Mater.* **2021**, *9*.

[24] G. M. Paternò, Q. Chen, X.-Y. Wang, J. Liu, S. G. Motti, A. Petrozza, X. Feng, G. Lanzani, K. Müllen, A. Narita, F. Scotognella, *Angew. Chem. Int. Ed.* **2017**, *56*, 6753–6757; *Angew. Chem.* **2017**, *129*, 6857–6861.

[25] G. M. Paternò, Q. Chen, R. Muñoz-Mármol, M. Guizzardi, V. Bonal, R. Kabe, A. J. Barker, P. G. Boj, S. Chatterjee, Y. Ie, J. M. Villalvilla, J. A. Quintana, F. Scotognella, K. Müllen, M. A. Díaz-García, A. Narita, G. Lanzani, *Mater. Horiz.* **2021**.

[26] M. G. Schwab, A. Narita, Y. Hernandez, T. Balandina, K. S. Mali, S. De Feyter, X. Feng, K. Mullen, *J. Am. Chem. Soc.* **2012**, *134*, 18169–18172.